

Mean-Field Theory for Diffusion-Limited Aggregation in Low Dimensions

Efim Brener,^(a) Herbert Levine, and Yuhai Tu

Department of Physics and Institute for Nonlinear Science, University of California, San Diego, La Jolla, California 92093

(Received 9 November 1990)

We present a new mean-field theory for diffusion-limited aggregation (DLA). We apply our approach to calculate the ensemble-averaged structure seen in recent experiments in a two-dimensional channel geometry. Our method explains the similarity between the average DLA occupancy and the Saffman-Taylor finger pattern.

PACS numbers: 68.70.+w, 47.15.Hg, 47.20.Hw

Diffusion-limited aggregation (DLA) is a stochastic model originally introduced by Witten and Sander¹ to describe tenuous structures. In this process, a cluster is grown via the attachment of random walkers released one at a time from a far distance. This approach has been very successful in simulating the formation of structures seen in electrochemical deposition² and unstable viscous fingering.^{3,4} Unfortunately, a theoretical framework for definitively analyzing simulation results has as yet proven elusive.

The relationship between DLA and the Saffman-Taylor viscous-finger problem⁵ was recognized several years ago.⁶ In the Saffman-Taylor (ST) case, growth is deterministically controlled by solving Laplace's equation for the pressure field; in DLA, the random-walker probability distribution obeys the selfsame Laplace equation, but the growth algorithm is intrinsically "noisy." Also, it is now understood that in the usual channel geometry, surface tension plays a crucial role in selecting the finger pattern and in determining its stability. One can use a "noise-reduced" DLA process which also includes surface tension to recover the ST finger;⁶ however, the irregular pattern seen in standard DLA (and in experiments) bears no obvious connection to a stable finger structure.

Recently, Arneodo *et al.* discovered a rather surprising feature of DLA in a channel geometry.⁷ By performing an ensemble average of the irregular patterns, they obtained the occupation probability distribution. Amazingly, the mean occupancy profile moves at constant speed and has the shape of the Saffman-Taylor pattern with finger width $\lambda=0.5$. This finger width is the selected structure determined by current theory in the small-surface-tension limit.⁵ This was found to be true both in DLA simulations and also in experiments involving unstable viscous fingering in a Hele-Shaw cell.

This paper is devoted to providing an explanation of these results via a new mean-field theory. A mean-field theory for DLA was originally proposed by Witten and Sander;⁸ this had the form

$$\frac{\partial \rho}{\partial t} = \nabla^2 u, \quad \frac{\partial \rho}{\partial t} = u(\rho + a^2 \nabla^2 \rho), \quad (1)$$

where ρ and u are the mean densities for "aggregates"

and "walkers," respectively, and a is the lattice spacing. The first equation is just the conservation of matter; the second equation implies the DLA growing law, i.e., the aggregates only grow when there are occupied neighbors and a random walker is available on the site. In an open space of dimension $d (> 2)$, this model predicts that the ρ profile goes like $1/r$, where r is the radial coordinate with the origin at the starting point, and the interface moves with constant velocity. This can be interpreted as giving rise to a fractal dimension $d_F = d - 1$.

It is easy to argue that these equations cannot be correct in a planar geometry. In the limit $a \rightarrow 0$, one can find a similarity solution by writing u and ρ as follows:

$$u(x, t) = xg[x(t_c - t)], \quad \rho(x, t) = x^{-2}f(x(t_c - t)) \quad (2)$$

$$(t < t_c),$$

where t_c is a finite critical time. Substituting into (1), the equations for g and f become

$$-f' = 2zg' + z^2g'' = gf, \quad (3)$$

where $z = x(t_c - t)$ and all the derivatives are with respect to z . The boundary condition for g is that g goes to a constant g_0 at infinity, corresponding to constant flux. It is not hard to solve these equations in the following two limiting regions: (1) when $z \gg 1$, $f(z) \sim \exp(-g_0 z)$, $g(z) \rightarrow g_0$; (2) when $z \ll 1$, $f(z) \rightarrow f_0$, $g(z) \sim z^\alpha$, with $\alpha = [(1 + 4f_0)^{1/2} - 1]/2$. This solution shows that the main part of the ρ profile behaves as $1/x^2$, a result first pointed out by Hakim.⁹ In a loose sense, the structure has negative dimension -1 and the front goes to infinity in a finite time t_c . A numerical simulation of Eq. (1) immediately verifies the $1/x^2$ power-law behavior and the concomitant interface acceleration. The same behavior will exist in a channel geometry, since the fields approach planar interface values sufficiently far in the front of the advancing structure.

The essential cause for the acceleration of the interface is the finite slope of the u field at infinity. Given this flux, any small fluctuation in front of the growing front will start to grow. In the actual DLA model, growth cannot occur with an infinitesimal fluctuation; instead the cluster must reach a particular point for

growth to occur and growth at occupation densities less than one occupied site must be suppressed. In other words, there should be a finite threshold in ρ to initiate growth, or at least a faster than linear vanishing of the growth rate at small ρ . The simplest way to accomplish this is to replace the first term in parentheses in Eq. (1), ρ , by ρ^γ with $\gamma > 1$. [This is certainly not the only way to introduce a cutoff, maybe not even the most natural way. However, we have used other types of cutoffs, e.g., instead of ρ^γ , we have also used the function $f(\rho)$: $f(\rho) = 0$ for $\rho < A$; $f(\rho) = \rho$ for $\rho > A$, where A is a small number. The results we obtained are qualitatively the same as those quoted here using ρ^γ .] It turns out that the basic physical nature of the model will not depend on γ as long as $\gamma > 1$.

So, the equations of the new mean-field model become

$$\frac{\partial \rho}{\partial t} = \nabla^2 u = u(\rho^\gamma + a^2 \nabla^2 \rho). \quad (4)$$

Again, we first consider the 1D planar problem. We rescale the problem as follows:

$$u = a^\gamma u_1, \quad \rho = a^{-\gamma} \rho_1, \quad x = a^\gamma x_1, \quad t = a^{\gamma-2} t_1. \quad (5)$$

Assuming there exists a steady-state solution with velocity v , we have

$$-v \rho_1' = u_1'' = u_1(\rho_1^\gamma + \rho_1''). \quad (6)$$

The derivatives are with respect to $z_1 = x_1 - vt_1$. Using the boundary condition that $\rho_1 \rightarrow 0$, $u_1' \rightarrow c$ (c is the flux of "walkers" fixed in the problem) at $z_1 \rightarrow \infty$, and defining $u_2 = u_1/v$, we have

$$u_2[(\rho_0 - u_2')^\gamma - u_2''] = u_2'', \quad (7)$$

where $\rho_0 = c/v$, with the boundary conditions $u_2 \rightarrow 0$, $u_2' \rightarrow 0$ as $z_1 \rightarrow -\infty$, and $u_2' \rightarrow \rho_0$ as $z_1 \rightarrow \infty$. Equation (7) is a third-order differential equation with three boundary conditions which is translation invariant; i.e., it does not contain any explicit dependence on z_1 . Simple counting arguments show that Eq. (7) is an eigenvalue equation for ρ_0 , which is the rescaled value of the uniform density far behind the growing front. We have solved Eq. (4) numerically for various γ (> 1). The density profiles all have "kink" fronts moving with constant velocity, and the shape of the profile is time independent after initial transients, as shown in Fig. 1. We have also directly solved the eigenvalue equation (7) numerically, and the values of ρ_0 agree very well with the simulation. The dependence of ρ_0 on γ can be roughly estimated by matching the asymptotic behaviors of the ρ and u fields; the result of this is that $\rho_0 \sim [(\gamma-1)/(\gamma+1)]q(\gamma)$, where $q(\gamma)$ is a slowly varying function of γ . As γ approaches 1, ρ_0 goes to 0, which means there is no steady-state solution for $\gamma = 1$.

Encouraged by the capability of this model to produce steady-state growth in 1D, we do the same simulation in the channel geometry with the boundary conditions in

the y direction: $\partial u / \partial y|_{y=\pm w/2} = 0$, $\rho|_{y=\pm w/2} = 0$. The structure of the equation makes the simulation quite straightforward. Given an initial distribution of ρ , we can solve Poisson's equation $(\nabla^2 - \rho^\gamma + a^2 \nabla^2 \rho)u = 0$; and from the distribution of u , $\partial \rho / \partial t$ is obtained, and the ρ field can be advanced in time. This is exactly the spirit of DLA: One releases another particle only when the previous one is absorbed by the aggregate. We also enforced symmetry about the center of the channel which is natural because we are averaging over many DLA runs.

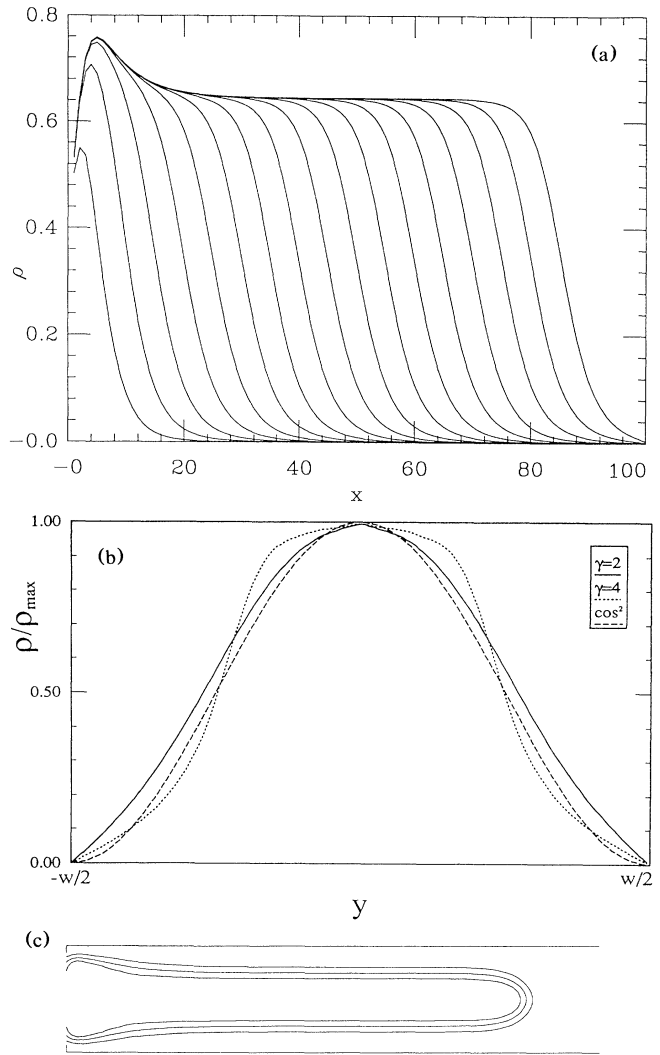


FIG. 1. Simulation results for $w=20$ and $a=1$. (a) Longitudinal profile of ρ at the center of the channel; (b) transverse profile of the normalized density for $\gamma=2, 4$, the dashed line is the function $\cos^2(\pi y/w)$. (c) Contour plot for the normalized density profile, the levels are 0.25, 0.5, and 0.75 from outer to inner; the 0.5 contour line is indistinguishable from the ST analytic solution for $\lambda=0.53$.

We have performed this simulation in lattices of sizes 20×100 and 40×100 for various values of γ and a . A steady-state solution was obtained for all $\gamma > 1$ and for all a . Figure 1(a) shows the density field ρ at the center of the channel versus the growing direction coordinate x , for different times. It is obvious from the graph that growth only occurs at the front, and behind the front, the density is constant after some initial transient. The transverse density profile is shown in Fig. 1(b). It has a maximum at the center and decreases to zero at the boundary, and the mid-height point is approximately at the midpoint between the center and the walls. The intermediate region between large-occupancy and small-occupancy regions becomes smaller with decreasing a and increasing γ . Finally, in Fig. 1(c) a contour line plot for the density field is presented for $a=1$ and $\gamma=2$. The $0.5\rho_{\max}$ line agrees very well with the Saffman-Taylor solution for $\lambda=0.53$. Both the mean occupancy profile and the transverse profile agree with the aforementioned experimental findings of Arneodo *et al.* For smaller a and larger γ , the $0.5\rho_{\max}$ contour lines approach ST solutions with λ closer to 0.5.

It has been well-known experimentally¹⁰ that the width of the stable finger in the Saffman-Taylor problem approaches 0.5 asymptotically as the surface tension goes to zero. However, it is only recently that it was understood that this phenomenon is due to surface tension acting as a singular perturbation.¹¹ The fact that the boundary of the large occupancy region in mean-field theory has the shape of the 0.5 Saffman-Taylor finger immediately raises the question: Is this behavior related to the selection mechanism of the Saffman-Taylor problem?

In order to answer the question, we first consider the limiting case where $\gamma \rightarrow \infty$ and $a \rightarrow 0$. The density field is divided into two regions: region (1), $\rho = \Delta\rho > 1$, then $\rho^\gamma \rightarrow \infty$, so $u=0$; region (2), $\rho=0$, so $\nabla^2 u=0$. On the boundary between the two regions, because of the conservation law ($\partial\rho/\partial t = \nabla^2 u$), we have $\Delta\rho v_n = -\mathbf{n} \cdot \nabla u$. Together with the boundary condition that $\partial u/\partial x \rightarrow c$ at $x \rightarrow \infty$, the mean-field equations become exactly the Saffman-Taylor equation at zero surface tension. For finite γ and a , the two regions ($u \approx 0$ and $\nabla^2 u \approx 0$) will be separated by a layer of finite width. Locally the problem can be approximately treated as a one-dimensional problem in the local-density gradient direction. According to the scaling in one dimension, the width of the layer is of order $O(a^\gamma)$, but because of the 2D nature of the problem, up to leading order, the Laplace operator ∇^2 equals $\partial^2/\partial n^2 + \kappa \partial/\partial n$, where n is the local gradient direction and κ is the local curvature of the front. So after scaling, compared to the one-dimensional problem, there are two extra terms, $a^\gamma \kappa u'_1$ and $a^\gamma \kappa \rho'_1$, present in the equation. Treating these two terms as perturbation, one can get effective boundary conditions for the Laplace equation. These boundary conditions will contain curvature terms and play the same stabilizing role as does the

surface energy in the ST problem. We therefore expect that singular perturbation caused by the Laplacian term will select the shape of the boundary layer to be approximately the 0.5 Saffman-Taylor finger.

The above argument can be tested by extending our calculations to the case of additional anisotropy. If the Laplacian term selects the observed large occupancy shape, then when anisotropy is introduced into the problem, the Laplacian term will select not the 0.5 Saffman-Taylor finger, but another solution of the family. Indeed, as we replace $\nabla^2 \rho$ by $\partial^2 \rho/\partial x^2 + b \partial^2 \rho/\partial y^2$, the shapes of the mean occupancy boundary fit very well with the Saffman-Taylor finger of different widths (Fig. 2), with the selected width λ an increasing function of the anisotropy parameter b . Our result agrees with experiments of Couder *et al.*,¹² where they also observed the Saffman-Taylor finger with different widths when anisotropy was introduced; however, a detailed correspondence between the theoretical and experimental ways of introducing anisotropy is not clear.

The action of the Laplacian in the mean-field theory as a sort of surface tension can be thought of in the following heuristic way. In a single DLA simulation, a site which has three neighbor sites being occupied and a site which has only one neighbor site being occupied will have the same ability to grow, so there is no surface tension. In a mean-field theory which is meant to describe the sum of many single DLA runs, a site which has a larger neighbor density will grow faster because the neighbor density consists of occupied sites from different runs and they do not block each other. Additional growth probability due to higher neighbor occupancy is essentially the spirit in which Kadanoff introduced surface tension into DLA simulations.⁶

As a final test of our approach, we investigate the dependence of the mean density profile far behind the front on the channel width w . Because of computer time limitations, simulations with very large w are not practical. But by rescaling the problem in the same way as in

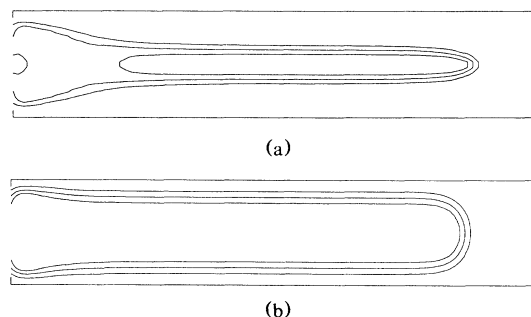


FIG. 2. Contour plots for the anisotropic cases: (a) $b=0.5$; the contour line for $\rho(x,y)/\rho_{\max}=0.25, 0.5$, and 0.75 are plotted, and the 0.5 line is fitted very accurately by the analytic ST solution for $\lambda=0.31$. (b) $b=2$; the 0.5 contour line matches the $\lambda=0.65$ ST solution.

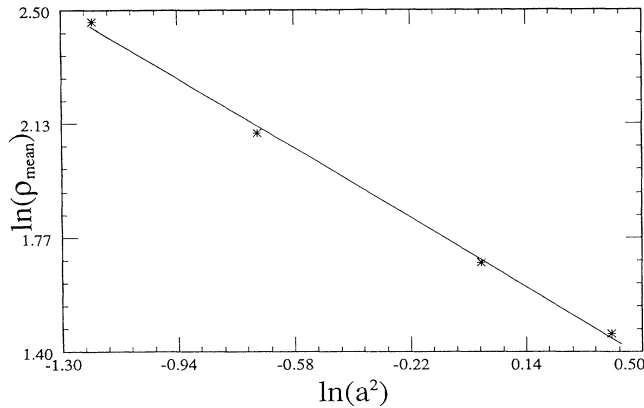


FIG. 3. Dependence of $\bar{\rho}$ on a^2 ; the plotted fit is $\bar{\rho} \sim a^\alpha$, with $\alpha \approx -1.26 \pm 0.06$.

1D, we find

$$\rho(x, y, w, a, \gamma) = a^{-2} P_\gamma(x/w, y/w, w/a^\gamma), \quad (8)$$

where P_γ is some function which depends on γ . Note that the channel width provides an extra length. The average occupancy is defined as

$$\bar{\rho} = w^{-2} \int_{-w/2}^{w/2} \int_{-w/2}^{w/2} \rho dx dy = a^{-2} S_\gamma(\omega/a^\gamma). \quad (9)$$

S_γ is another function depending on γ . This scaling form allows us to vary a instead of w and from the dependence of $\bar{\rho}$ on a , its dependence on w is obvious. We show in Fig. 3 the dependence of $\bar{\rho}$ on a^2 for $\gamma=2$, from that we get $\bar{\rho} \sim w^\mu/a^\omega$, with $\mu = -0.36 \pm 0.03$ and $\omega = 1.28 \pm 0.06$. The value of μ , the roughness exponent, is very close to the one measured in the experiment. We have checked that the exponent is insensitive to the value of γ , at least within the range $1.5 < \gamma < 2$. This agreement is somewhat remarkable; it suggests that the mean-field-theory approach might provide a method for quantitatively estimating the DLA fractal exponent, though perhaps not determining it exactly.

We should point out there is one problem with our purely deterministic mean-field theory in the channel geometry. In the experiment, the tip region spreads as \sqrt{t} , a result which is absent from our simulation. This difficulty might be resolved by recognizing that the x location of the density front is a marginal mode which will acquire dynamics when fluctuations around the mean field are taken into account. Exactly how to do this in a consistent manner will require further investigation.

In conclusion, we have modified the mean-field theory for DLA growing in low dimension, and derived results

in good agreement with experiment findings. We argue that the Laplacian term $\nabla^2 \rho$ in the growth equation plays the same role in selecting the shape of the large occupancy region as surface tension in the problem of viscous-finger growth. The additional parameter γ which appears in the theory should probably be interpreted as a cutoff, with the actual DLA answer being given by the limit $\gamma \rightarrow 1^+$; whether the different transverse profile seen in the viscous-fingering data could be explained by having $\gamma > 1$ is unclear at this point. Finally, we also have applied our model to growth in a two-dimensional sector geometry and will report the results elsewhere.

This work was supported in part by the U.S. Defense Advanced Projects Administration under the University Research Initiative, Grant No. N00014-86-K-0758.

^(a)Permanent address: Institute for Solid-State Physics of the Academy of Sciences of the U.S.S.R., Chernogolovka, Moscow District, U.S.S.R.

¹T. A. Witten and L. M. Sander, Phys. Rev. Lett. **47**, 1400 (1981).

²Y. Sawada, A. Dougherty, and J. Gollub, Phys. Rev. Lett. **56**, 1260 (1986); D. Grier, E. Ben-Jacob, R. Clarke, and L. Sander, Phys. Rev. Lett. **56**, 1264 (1986).

³S. N. Raouso, P. D. Barnes, and J. V. Maher, Phys. Rev. A **35**, 1245 (1987).

⁴Y. Couder, in *Random Fluctuation and Pattern Formation*, edited by H. E. Stanley and N. Ostrowsky (Kluwer, Dordrecht, 1988).

⁵For review of the field of interfacial pattern formation, see D. Kessler, J. Koplik, and Herbert Levine, Adv. Phys. **37**, 255 (1988); J. S. Langer, in *Chance and Matter*, edited by J. Souletie (North-Holland, Amsterdam, 1987).

⁶L. P. Kadanoff, J. Stat. Phys. **39**, 267 (1985); D. Bensimon, L. P. Kadanoff, S. Liang, B. I. Shraiman, and C. Tang, Rev. Mod. Phys. **50**, 977 (1986).

⁷A. Arneodo, Y. Couder, G. Grasseau, V. Hakim, and M. Rabaud, Phys. Rev. Lett. **63**, 984 (1989).

⁸T. Witten and L. M. Sander, Phys. Rev. B **27**, 5686 (1983); R. Ball, M. Nauenberg, and T. A. Witten, Phys. Rev. A **29**, 2019 (1984).

⁹V. Hakim (private communication).

¹⁰P. G. Saffman and G. I. Taylor, Proc. Roy. Soc. London A **245**, 312 (1958); P. Tabeling and A. Libchaber, Phys. Rev. A **33**, 794 (1986).

¹¹B. I. Shraiman, Phys. Rev. Lett. **56**, 2028 (1986); D. Hong and J. S. Langer, Phys. Rev. Lett. **56**, 2032 (1986); R. Combescot, T. Dombre, V. Hakim, Y. Pomeau, and A. Pumir, Phys. Rev. Lett. **56**, 2036 (1986).

¹²Y. Couder, F. Argoul, A. Arneodo, J. Maurer, and M. Rabaud, Phys. Rev. A **42**, 3499 (1990).